

Droplet microfluidics for amplification-free genetic detection of single cells

Tushar D. Rane^a, Helena Zec^a, Chris Puleo^a, Abraham P. Lee^b and Tza-Huei Wang^{*a,c}

SUPPLEMENTAL DATA

S.1 Droplet volume and its effect on the target concentration within the droplet

Target Molecules per droplet	20000	
Droplet diameter (µm)	Droplet volume (pL)	Target concentration in droplet (nM)
15	1.77	1.88E+01
25	8.18	4.06E+00
35	22.45	1.48E+00
50	65.45	5.07E-01
75	220.89	1.50E-01
100	523.60	6.34E-02
1000	523598.78	6.34E-05

Supp. Table 1: Table illustrating the effect of droplet volume on target concentration within the droplet

The following table illustrates the concentrating power of droplets with respect to single cells. In this table, we assume that an intracellular target of interest is present at the concentration of 20000 targets per cell. This number is well within the range of 16s rRNA count per *E. coli* cell^{1, 2}. The table shows how the concentration of the same number of target molecules (from a single cell) changes from nanomolar to femtomolar concentrations depending on the volume in which they are released.

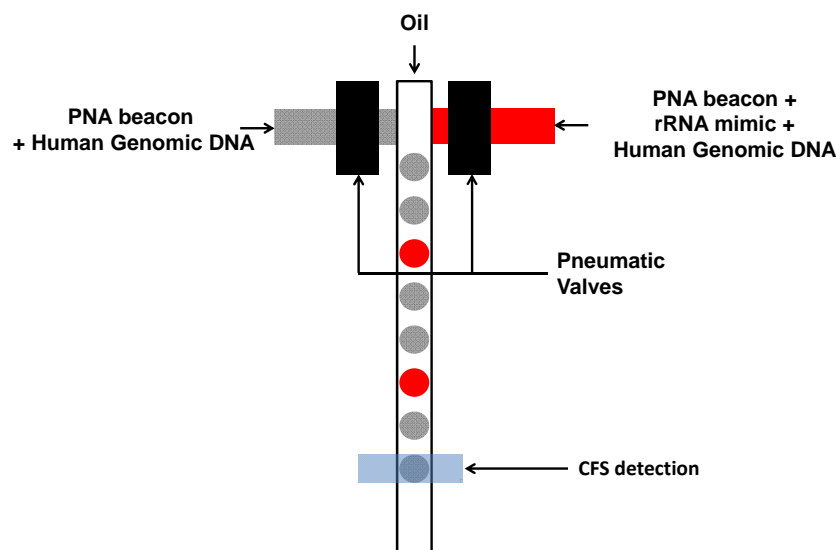
S.2 Device design and fabrication for experiments with 16s rRNA mimic

We designed a dual layer PDMS device for our experiments with the rRNA mimic. The schematic illustrating the operation of this device is shown in Supp. Fig. 1. The device consisted of one oil inlet and two sample inlets. One of the sample inlets took the 'positive control' (PNA beacon + rRNA mimic + Human Genomic DNA) as input while the other sample inlet took the 'negative control' (PNA beacon + Human Genomic DNA) as input, according to the description in the article text. Both of these sample inlets are separated from the oil flow channel through two valves. These valves are fabricated using standard multilayer soft lithography as has been described previously³. The actuation of these valves can be controlled using custom software written in MatlabTM. Alternating actuation of these valves was used to generate droplet trains consisting of different proportions of droplets generated from the positive and negative control samples. The droplet train thus generated simulates the train of droplets we expect to be generated while working with a cell sample i.e. a series of droplets with (positive) and without cells (negative) encapsulated in them. These droplet trains are then routed to a downstream detection region on chip, where fluorescence detection is conducted through Confocal Fluorescence Spectroscopy.

S.3 Fluorescence data analysis for experiments with 16s rRNA mimic

Both the positive and negative control samples being input to the device described above in S.2 had an indicator dye (Alexa 488 10nM) added to them for identification of the droplet region in the oil background from the fluorescence data collected from the droplet train. Custom software written in MatlabTM was used for processing the raw fluorescence data. As described in the article,

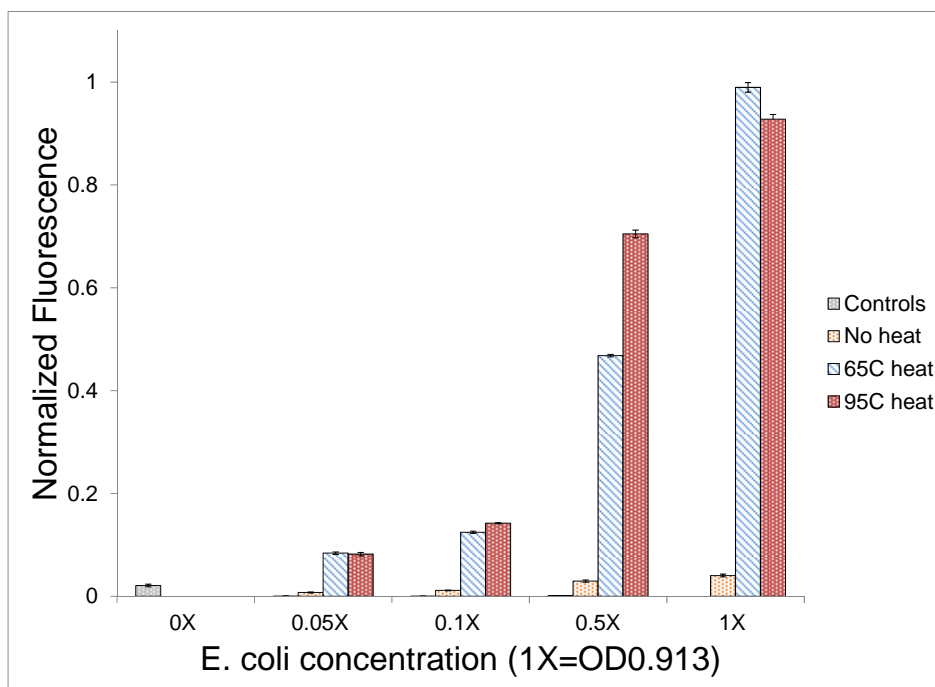
our fluorescence setup is capable of dual excitation with a 488nm and a 633nm wavelength laser. The fluorescence collected from the sample excited by these lasers is then split into two wavelength bands centered at 520nm (Green) and 670nm (Red). Fluorescence intensity from these two wavelength bands is sensed by two individual avalanche photodiodes and converted into photon counts per unit time using custom software written in LabVIEW. The fluorescence signal in the green band is due to the fluorescence of the indicator dye while the fluorescence in the red band is from the Cy5 dye on the PNA beacon. Initially the droplet region for each individual droplet is identified from the fluorescence signal trace corresponding to the green band by setting a threshold on fluorescence intensity. Varying this threshold doesn't have much effect on identification of the droplet region due to uniform fluorescence intensity of the indicator dye encapsulated within the droplets. The photons in the red band from the region corresponding to each individual droplet were then summed to obtain a burst size for each droplet. This burst size was normalized to a standard droplet size to overcome any bias due to small size differences in different droplets. Since the droplet sequence in the droplet train was known, first 10 control sample droplets were used to set a threshold for differentiating between 'positive' and 'negative' droplets. Specifically the threshold was set at a stringent [burst size mean + 20* (burst size standard deviation)] to differentiate between positive and negative droplets. This stringent threshold prevented any false positives occurring due to small fluctuations in the fluorescence intensity of 'negative' droplets over time. For each different droplet train, three batches of 100 droplets each were analyzed to obtain a positive droplet count per 100 droplets. The mean and standard deviation obtained from this analysis was then plotted as shown in Fig. 4 in the article.



Supp. Fig. 1: Schematic of the chip design for experiments with 16s rRNA mimic

S.4 Optimizing the incubation temperature for the PNA beacon assay in bulk

Prior to our experiments with *E. coli* cell samples on chip, we conducted some experiments in bulk to optimize the temperature incubation conditions for the assay with live cell samples. Briefly we mixed different quantities of *E. coli* cells with PNA beacon and incubated them at different temperatures. Fluorescence detection was then conducted on these samples using Confocal Fluorescence Spectroscopy (CFS). PNA beacon hybridization with complementary target (16S rRNA) released after lysis of the *E. coli* cells leads to increase in fluorescence collected from a sample. We tested three different temperatures viz. Room Temperature (RT), 65°C and 95°C. The results shown in Supp. Fig. 2 indicate that the cell lysis and PNA hybridization was inefficient at RT incubation. Incubation at 65°C and 95°C on the other hand resulted in comparable cell lysis and PNA hybridization efficiency. We used 65°C incubation for our experiments on chip to prevent any possible problems with droplet evaporation or instability due to high temperature incubation.



Supp. Fig. 2: Effect of incubation temperature on the cell lysis and PNA beacon hybridization efficiency

Notes and References

^aDepartment of Biomedical Engineering, Johns Hopkins University, Baltimore, USA.; Tel: +1 410 5164746

^bDepartment of Biomedical Engineering, University of California, Irvine, Irvine, USA.; Tel: +1 949 824 9691

^cDepartment of Mechanical Engineering, Johns Hopkins University, Baltimore, USA.; Tel: +1 410 516 7086; E-mail: thwang@jhu.edu

1 K. Zwirgmaier, W. Ludwig and K. H. Schleifer, *Mol. Microbiol.*, 2004, **51**, 89-96.

2 T. Hoshino, L. S. Yilmaz, D. R. Noguera, H. Daims and M. Wagner, *Appl. Environ. Microbiol.*, 2008, **74**, 5068-5077 (DOI:10.1128/AEM.00208-08).

3 T. D. Rane, C. M. Puleo, K. J. Liu, Y. Zhang, A. P. Lee and T. H. Wang, *Lab. Chip*, 2010, **10**, 161-164 (DOI:10.1039/b917503b).